

Midrapidity Hyperon Production in pp and pA Collisions

G.H. Arakelyan, C. Merino, and Yu.M. Shabelski

Presented by C. Merino at Initial Stages 2014 (IS2014)

*The 2nd International Conference on the
Initial Stages in High-Energy Nuclear Collisions
Napa Valley, CA, USA, 3-7 December, 2014*

Abstract In this paper we present the description of the production of strange and mulistrange baryons in a wide energy region, from CERN SpS up to LHC, in the framework of the Quark-Gluon String model.

The Quark-Gluon String model (QGSM) [1, 2, 3] is built on the Dual Topological Unitarization, nonperturbative notions of QCD, and Regge Theory based phenomenology. The QGSM has been successfully used for the description of multiparticle production processes in hadron-hadron [4, 5] and hadron-nucleus [6] collisions. In the case of interaction with a nuclear target, the Multiple Scattering Theory (Gribov-Glauber Theory) is implemented.

Though it is not the direct aim of the present paper, one has to note that such an approach based on the analysis of Feynman and reggeon diagrams has been already used [7, 8] to study the anisotropic flows, and, in particular, the elliptic flow v_2 in collisions of hadrons and nuclei at high energies, questions so extensively discussed during this conference.

The significant differences observed in the yields of baryons and antibaryons in the central (midrapidity) region are connected with [3, 9] the special structure of

G.H. Arakelyan

A.Alikhanyan National Scientific Laboratory (Yerevan Physics Institute), Yerevan, 0036, Armenia.
e-mail: argev@mail.yerphi.am

C. Merino

Departamento de Física de Partículas, Facultade de Física and Instituto Galego de Física de Altas Enerxías (IGFAE), Universidade de Santiago de Compostela, Santiago de Compostela 15782, Galiza, Spain. e-mail: carlos.merino@usc.es

Yu.M. Shabelski

Petersburg Nuclear Physics Institute, NCR Kurchatov Institute, Gatchina, St.Petersburg 188350, Russia. e-mail: shabelsk@thd.pnpi.spb.ru

baryons, consisting of three valence quarks together with a special configuration of the gluon field, called String Junction [10].

At very high energies, the contribution of the enhancement Reggeon diagrams becomes important, leading to the suppression of the inclusive density of secondaries [11] in the central (midrapidity) region.

The relative probabilities for the production of various baryons depend on the universal suppression factor S/L , for which we take the value, $S/L = 0.32$ [12], and they can be found on the basis of simple combinatorial analysis of quarks [13, 14].

In QGSM the inclusive spectrum of a secondary hadron h is determined by the convolution of the diquark, valence quark, and sea quark distributions, $u(x, n)$, in the incident particles, with the fragmentation functions, $G^h(z)$, of quarks and diquarks into the secondary hadron h [1, 2]. Both the distributions and the fragmentation functions are constructed by using the Reggeon counting rules [15].

For the case of interaction with a nucleus, it is technically more simple [16, 17] to consider the maximal number of Pomerons, n_{max} , emitted by one nucleon in the central region that can be cut. In this frame, we obtain a reasonable agreement with the experimental data on the inclusive spectra of secondaries produced in p+Pb collisions at LHC energy [17] with the value $n_{max} = 23$. It has been shown in [18] that the number of strings that can be used for the secondary production should increase with the initial energy.

The QGSM fragmentation formalism allows one to calculate the integrated over p_T spectra of different secondaries as the functions of rapidity and x_F , the accuracy of these calculations being of about 10%.

In Table 1, and in figs. 1 and 2, we compare the existing experimental data on the energy dependence until LHC energies integrated over the whole range of p_T for Λ , $\bar{\Lambda}$, Ξ^- , and $\bar{\Xi}^+$ hyperons production density, dn/dy ($|y| \leq 0.5$), in pp (upper panel in Fig. 1) [19-27] and pA [28-31] (lower panel in Fig. 1, and Fig. 2) collisions to the corresponding results obtained by the QGSM.

In Fig. 1 we also present the QGSM prediction for the energy dependence of the Ω^- and $\bar{\Omega}^+$ hyperon production until LHC energies.

As one can see in Fig. 1, the absolute values of the densities $dn/dy(|y| \leq 0.5)$ for Λ , $\bar{\Lambda}$ production are one order of magnitude higher than for Ξ^- and $\bar{\Xi}^+$ in a large energy region up to the LHC range. The same is also true for Ω^- and $\bar{\Omega}^+$ densities when compared to those of Ξ^- and $\bar{\Xi}^+$.

\sqrt{s} (GeV)	Reaction	QGSM	Experiment dn/dy ($ y \leq 0.5$)
13.97 (102 GeV/c)	$p + p \rightarrow \Lambda$	0.025	0.012 ± 0.01 [19]
14.075 (147 GeV/c)	$p + p \rightarrow \Lambda$	0.025	0.0090 ± 0.0015 [20]
14.075 (147 GeV/c)	$p + p \rightarrow \bar{\Lambda}$	0.010	0.057 ± 0.0044 [20]
19.42 (200 GeV/c)	$p + p \rightarrow \Lambda$	0.026	0.0106 ± 0.006 [21]
19.42 (200 GeV/c)	$p + p \rightarrow \bar{\Lambda}$	0.011	0.007 ± 0.0015 [21]
19.66 (205 GeV/c)	$p + p \rightarrow \Lambda$	0.026	0.015 ± 0.0044 [22]
23.76 (300 GeV/c)	$p + p \rightarrow \Lambda$	0.026	0.0076 ± 0.006 [23]
23.76 (300 GeV/c)	$p + p \rightarrow \bar{\Lambda}$	0.013	0.015 ± 0.0076 [23]
27.6 (405 GeV/c)	$p + p \rightarrow \Lambda$	0.027	0.0091 ± 0.0045 [24]
27.6 (405 GeV/c)	$p + p \rightarrow \bar{\Lambda}$	0.015	0.017 ± 0.0041 [24]
200.	$p + p \rightarrow \Lambda$	0.045	$0.0436 \pm 0.0008 \pm 0.004$ [25]
200.	$p + p \rightarrow \bar{\Lambda}$	0.039	$0.0398 \pm 0.0008 \pm 0.0037$ [25]
200.	$p + p \rightarrow \Lambda(FD)$	0.045	$0.0385 \pm 0.0007 \pm 0.0035$ [25]
200.	$p + p \rightarrow \bar{\Lambda}(FD)$	0.039	$0.0351 \pm 0.0007 \pm 0.0032$ [25]
200.	$p + p \rightarrow \Xi^-$	0.005	$0.0026 \pm 0.0002 \pm 0.0009$ [25]
200.	$p + p \rightarrow \bar{\Xi}^+$	0.005	$0.0029 \pm 0.0003 \pm 0.006$ [25]
200.	$p + p \rightarrow \Omega^- + \bar{\Omega}^+$	0.001	$0.00034 \pm 0.00016 \pm 0.0005$ [25]
900.	$p + p \rightarrow \Lambda$	0.065	0.26 ± 0.01 [26]
7000.	$p + p \rightarrow \Lambda$	0.099	0.27 ± 0.01 [26]
900.	$p + p \rightarrow \Lambda$	0.065	$0.108 \pm 0.001 \pm 0.012$ [27]
7000.	$p + p \rightarrow \Lambda$	0.099	$0.189 \pm 0.001 \pm 0.022$ [27]
900.	$p + p \rightarrow \Xi^-$	0.009	$0.011 \pm 0.001 \pm 0.001$ [27]
7000.	$p + p \rightarrow \Xi^-$	0.015	$0.021 \pm 0.001 \pm 0.003$ [27]

Table 1: Experimental data for strange baryons and antibaryons production in pp collisions at different energies, from CERN SpS up to LHC, together with the corresponding description by the QGSM.

\sqrt{s} (GeV)	Reaction	QGSM	Experiment dn/dy ($ y \leq 0.5$)
19.42 (200 GeV/c)	$p + \text{Ar} \rightarrow \Lambda$	0.042	0.025 ± 0.01 [28]
19.42 (200 GeV/c)	$p + \text{Xe} \rightarrow \Lambda$	0.052	0.05 ± 0.015 [28]
19.42 (200 GeV/c)	$p + \text{Au} \rightarrow \Lambda$	0.055	0.05 ± 0.01 [29]
19.42 (200 GeV/c)	$p + \text{Au} \rightarrow \bar{\Lambda}$	0.021	0.013 ± 0.06 [29]
19.42 (200 GeV/c)	$p + \text{S} \rightarrow \Lambda$	0.041	0.06 ± 0.005 [30]
19.42 (200 GeV/c)	$p + \text{S} \rightarrow \bar{\Lambda}$	0.016	0.015 ± 0.0025 [30]
17.2 (m.b.)	$p + \text{Be} \rightarrow \Lambda$	0.033	$0.034 \pm 0.0005 \pm 0.003$ [31]
	$p + \text{Be} \rightarrow \bar{\Lambda}$	0.011	$0.011 \pm 0.0002 \pm 0.001$ [31]
17.2 (m.b.)	$p + \text{Pb} \rightarrow \Lambda$	0.055	$0.060 \pm 0.002 \pm 0.006$ [31]
	$p + \text{Pb} \rightarrow \bar{\Lambda}$	0.019	$0.015 \pm 0.001 \pm 0.002$ [31]

Table 2: Experimental data for strange baryons and antibaryons production in proton-nucleus collisions at different energies, together with the corresponding description by the QGSM.

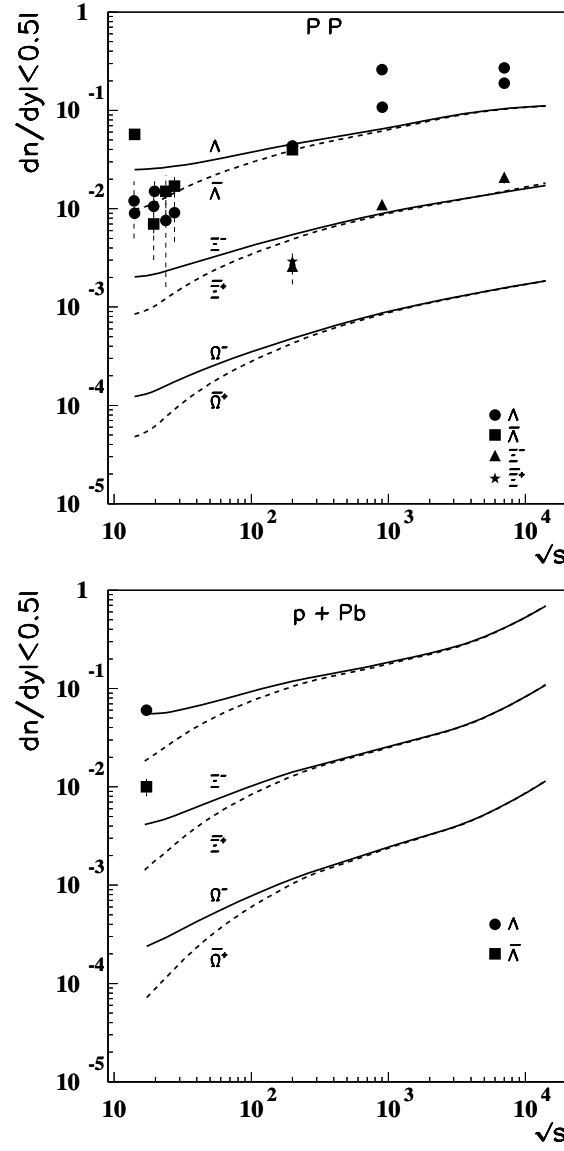


Fig. 1 Experimental data, integrated over p_T , on the energy dependence of hyperon production in midrapidity region for pp (upper panel) and p+Pb (lower panel) collisions, compared to the corresponding QGSM calculations (baryons are shown by full curves and antibaryons by dashed curves).

As one can see, both in figs. 1 and 2 and in Table 1, the experimental data on $dn/dy(|y| \leq 0.5)$ obtained by different collaborations are not thoroughly compatible among them, what it is probably due to different experimental event selec-

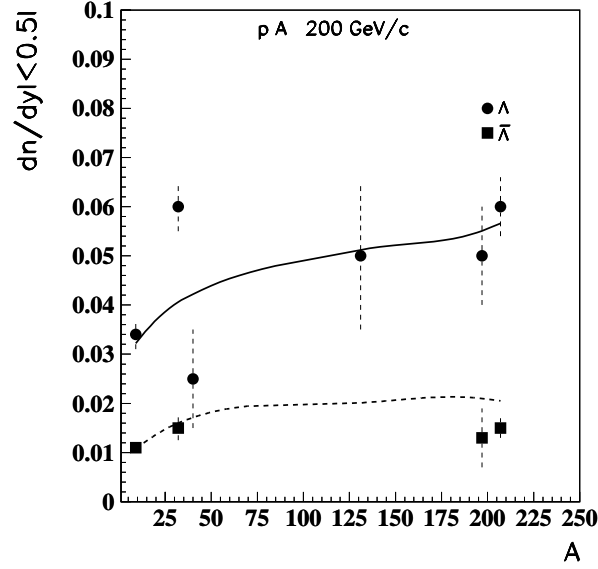


Fig. 2 Experimental data, integrated over p_T , on the A-dependence of the midrapidity density of Λ and $\bar{\Lambda}$ hyperons produced at 200 GeV/c [28, 29, 30, 31], compared to the corresponding QGSM calculations (baryons are shown by full curves and antibaryons by dashed curves).

tions, especially when comparing measurements by CMS and ATLAS collaborations. Nonetheless, the agreement of the QGSM results with the different sets of experimental data is good enough when compared to those experimental discrepancies.

In Fig. 2 the A-dependences of Λ and $\bar{\Lambda}$ hyperons produced on nuclear targets [28, 29, 30, 31] are shown. Also here the QGSM curves are in a reasonable agreement with the experimental data.

Acknowledgements

C.M. wants to congratulate the organizers for getting the scientifically exciting environment that it has made this conference so fruitful.

We thank C. Pajares for useful discussions. This paper was supported by Ministerio de Economía y Competitividad of Spain (FPA2011-22776), the Spanish Consolider-Ingenio 2010 Programme CPAN (CSD2007-00042), by Xunta de Galicia, Spain (2011/PC043), by the State Committee of Science of the Republic of Armenia (Grant-13-1C023), and by Russian RSCF grant No.14-22-00281.

References

1. A.B. Kaidalov and K.A. Ter-Martirosyan, *Yad. Fiz.* **39**, 1545 (1984); **40**, 211 (1984).
2. A.B. Kaidalov, *Sov. J. Nucl. Phys.* **66**, 1994 (2003); *Yad. Fiz.* **66**, 2014 (2003).
3. G.H. Arakelyan, A. Capella, A.B. Kaidalov, and Yu.M. Shabelski, *Eur. Phys. J.* **C26**, 81 (2002) and hep-ph/0103337.
4. G.H. Arakelyan, C. Merino, C. Pajares, and Yu.M. Shabelski, *Eur. Phys. J.* **C54**, 577 (2008) and hep-ph/0709.3174.
5. C. Merino, C. Pajares, and Yu.M. Shabelski, *Eur. Phys. J.* **C71**, 1652 (2011).
6. A.B. Kaidalov, K.A. Ter-Martirosyan, and Yu.M. Shabelski, *Yad. Fiz.* **43**, 1282 (1986).
7. K.G. Boreskov, A.B. Kaidalov, O.V. Kancheli, *Eur. Phys. J.* **C58**, 445 (2008) and arXiv:0809.0625[hep-ph].
8. K.G. Boreskov, A.B. Kaidalov, O.V. Kancheli, *Phys. Atom. Nucl.* **72**, 361 (2009); *Yad. Fiz.* **72**, 390 (2009).
9. C. Merino, M.M. Ryzhinski, and Yu.M. Shabelski, *Eur. Phys. J.* **C62**, 491 (2009).
10. G.C. Rossi and G. Veneziano, *Nucl. Phys.* **B123**, 507 (1977).
11. A. Capella, A. Kaidalov, and J. Tran Thanh Van, *Heavy Ion Phys.* **9**, 169 (1999).
12. G.H. Arakelyan, A.B. Kaidalov, C. Merino, and Yu.M. Shabelski, *Phys. Atom. Nucl.* **74**, 126 (2011) and arXiv:1004.4074[hep-ph].
13. V.V. Anisovich and V.M. Shekhter, *Nucl. Phys.* **B55**, 455 (1973).
14. A. Capella and C.A. Salgado, *Phys. Rev.* **C60**, 054906 (1999).
15. A.B. Kaidalov, *Sov. J. Nucl. Phys.* **45**, 902 (1987); *Yad. Fiz.* **43**, 1282 (1986).
16. C. Merino, C. Pajares, and Yu.M. Shabelski, *Eur. Phys. J.* **C59**, 691 (2009) and arXiv:0802.2195[hep-ph].
17. C. Merino, C. Pajares, and Yu.M. Shabelski, arXiv:1207.6900[hep-ph].
18. J. Dias de Deus and C. Pajares, *Phys. Lett.* **B695**, 211 (2012) and arXiv:1011.1099[hep-ph].
19. J.W. Chapman *et al.*, *Phys. Lett* **B47**, 465 (1975).
20. D. Brick *et al.*, *Nucl. Phys.* **B164**, 1 (1980).
21. F. Lopinto *et al.*, *Phys. Rev.* **D22**, 323 (1980).
22. K. Jaeger *et al.*, *Phys. Rev.* **D11**, 2405 (1975).
23. A. Sheng *et al.*, *Phys. Rev.* **D11**, 722 (1975).
24. H. Kichimi *et al.*, *Phys. Rev.* **D20**, 37 (1979) and arXiv:1111.1297[hep-ex].
25. B. Abelev *et al.*, STAR Collaboration, *Phys. Rev.* **C75**, 064901 (2011) and arXiv:06007033[nucl-ex].
26. G. Aad *et al.*, ATLAS Collaboration, *Phys. Rev.* **D85**, 012001 (2012).
27. V. Khachatryan *et al.*, CMS Collaboration, *JHEP* **05**, 064 (2011) and arXiv:1102.4282[hep-ex].
28. E. Derado *et al.*, NA5 Collaboration, *Z. Phys.* **C50**, 31 (1991).
29. A. Bamberger *et al.*, NA35 Collaboration, *Z. Phys.* **C41**, 25 (1989).
30. J. Bartke *et al.*, NA35 Collaboration, *Z. Phys.* **C48**, 191 (1990).
31. F. Antinori *et al.*, NA57 Collaboration, *J. Phys.* **G32**, 427 (2006) and arXiv:0601021[nucl-ex].